Ultrasonic attenuation in electron-hole liquids

Makio Uwaha*
Department of Physics and Materials Research Laboratory, University of Illinois at Urbana-Champaign, Urbana, Illinois 61801 and Institut Laue-Langevin, Boîte Postale 156X, 38042 Grenoble Cédex, France

Gordon Baym
Department of Physics, University of Illinois at Urbana-Champaign, 1110 West Green Street, Urbana, Illinois 61801
(Received 5 April 1985; revised manuscript received 4 April 1986)

A theory of the attenuation of longitudinal sound in electron-hole liquids in semiconductors, based on coupled electron and hole kinetic equations, is developed. The theory takes into account the existence of several bands of Fermi liquids, with differing charge and interaction with the lattice, the fact that the Fermi wave numbers are so small that the wave number of the sound can exceed them, and the effects of intraband collisions, which can be rapid enough to produce a significant reduction in the attenuation, even in the high-frequency regime. The theory is applied to sound propagating in the ⟨111⟩ direction in a Ge electron-hole liquid, and the ⟨100⟩ direction in a Si liquid. The former case, compared with the recent experiments by Dietsche, Kirch, and Wolfe [Phys. Rev. B **26**, 780 (1982)], suggests that intraband collisions play an important role in the sound-attenuation process.

I. INTRODUCTION

Recent advances in phonon spectroscopy have made it possible to use ultrasound as a useful probe of the properties of electron-hole liquids in semiconductors.[1] The aim of this paper is to present the basic framework of the theory of sound propagation in these systems.

The problem of sound propagation in electron-hole liquids in semiconductors differs from that in normal metals[2,3] in several important ways. The electron-hole liquids[4] are characterized by being a multiple-component degenerate system, with two different charge states, and several filled valleys in the band structure for each charge component. The electrons and the holes in different valleys react to the sound in different ways and their motions are correlated due to their mutual interactions. In normal metals the ionic charge is compensated by the conduction electrons. Here, however, the ions are effectively neutral, and instead the electron and hole charges compensate each other. The second feature distinguishing this problem from that in ordinary metals is that the Fermi wave numbers of the components are relatively small, on the order of 10^6–10^7 cm^{-1}. As a consequence, one can experimentally study propagation of sound of wavelengths shorter than the Fermi wavelength k_F^{-1} using modern techniques of phonon spectroscopy.

In the present problem electron-lattice scattering processes can generally be neglected, unlike in a normal metal, where they play an essential role in ultrasonic attenuation.[5] On the other hand, intraband electron-electron and hole-hole collision times may be short enough to be comparable to the sound frequency, even at wavelengths on the order of k_F^{-1}. While these relaxation times[5,6] are not well enough known presently to enable one to make a detailed comparison between the predicted and observed attenuation, attenuation experiments do allow one to estimate the order of magnitude of these collision times.

The general approach we use is that of coupled electron and hole kinetic equations, with the interaction with sound described by deformation potentials. We concentrate here on longitudinal sound propagation; the extension to transverse sound is straightforward, although more involved technically. In Sec. II we illustrate the method and physical features by dealing with a model with the simplest band structure. Applications to more realistic systems are given in Sec. III, where we mainly discuss the attenuation of longitudinal sound in the electron-hole liquid of Ge propagating along the ⟨111⟩ direction, and in Si along the ⟨100⟩ direction. A comparison with the recent experiments on Ge by Dietsche, Kirch, and Wolfe,[1] which show smaller attenuation than the value one expects from a simple perturbation-theory calculation, suggests that the effect of intraband collisions is very important.

II. ULTRASONIC ATTENUATION IN A SIMPLE ELECTRON-HOLE LIQUID

In order to present the physical picture clearly, we first discuss an idealized system with the simplest band structure: a direct-gap semiconductor with isotropic, nondegenerate bands. We introduce our model in subsection A, describe the motion of electrons and holes by kinetic equations in subsection B, and compute their reaction to the lattice and the related self-energy of a phonon propagating in the electron-hole liquid in subsection C. The physical interpretation of the results is discussed in subsection D.

A. Interaction between electrons, holes, and ions

We first consider the forms of the various interactions between electrons, holes, and ions. We describe the electron-ion interaction by a deformation potential.[7] The explicit form of the energy functional we assume is the following:

$$E=E_{\rm ion}[\dot{u}_\mu(\mathbf{r}),u_{\mu\nu}(\mathbf{r})]+\tfrac{1}{2}\int d^3r\int d^3r'\,\frac{e^2}{\kappa}\frac{[n_e(\mathbf{r})-n_h(\mathbf{r})][n_e(\mathbf{r}')-n_h(\mathbf{r}')]}{|\mathbf{r}-\mathbf{r}'|}$$
$$+\int d^3r\int d\Lambda[n_{\rm p}^e(\mathbf{r})\varepsilon_{1,\rm p}^e(u_{\mu\nu}(\mathbf{r}))+n_{\rm p}^h(\mathbf{r})\varepsilon_{1,\rm p}^h(u_{\mu\nu}(\mathbf{r}))]\,, \tag{2.1}$$

where $E_{\rm ion}[\dot{u}_\mu(\mathbf{r}),u_{\mu\nu}(\mathbf{r})]$ is the ion elastic plus kinetic energy in terms of the ion displacement field $u_\mu(\mathbf{r})$ and the strain $u_{\mu\nu}(\mathbf{r})$; $\varepsilon_{1,\rm p}^{e\,(h)}(u_{\mu\nu})$ is the single-electron (or -hole) energy with momentum $\mathbf{p}$ in the presence of a strain $u_{\mu\nu}$, without the long-range Coulomb potential, and $n_{\rm p}^{e\,(h)}$ is the distribution function of these states. The sign of the hole energy $\varepsilon_{1,\rm p}^h$ follows the usual convention of being measured downward. Here $d\Lambda=2\,d^3p/(2\pi\hbar)^3$, where the factor of 2 comes from the spin degree of freedom. The number density of the electrons (or holes) is given by

$$n_{e\,(h)}(\mathbf{r})=\int d\Lambda\, n_{\rm p}^{e\,(h)}(\mathbf{r})\,. \tag{2.2}$$

The single-particle energies of the electrons $\varepsilon_{\rm p}^e(\mathbf{r})$ and of the holes $\varepsilon_{\rm p}^h(\mathbf{r})$, including the electron and hole interactions, are obtained as

$$\varepsilon_{\rm p}^e(\mathbf{r})=\frac{\delta E}{\delta n_{\rm p}^e}=\varepsilon_{1,\rm p}^e(\mathbf{r})+e\phi(\mathbf{r})\,,$$
$$\varepsilon_{\rm p}^h(\mathbf{r})=\frac{\delta E}{\delta n_{\rm p}^h}=\varepsilon_{1,\rm p}^h(\mathbf{r})-e\phi(\mathbf{r})\,, \tag{2.3}$$

where e is the electron charge and the potential $\phi(\mathbf{r})$ is

$$\phi(\mathbf{r})=\int d^3r'\frac{e}{\kappa}\frac{n_e(\mathbf{r}')-n_h(\mathbf{r}')}{|\mathbf{r}-\mathbf{r}'|}\,. \tag{2.4}$$

The forces acting on the electrons, $\mathbf{F}_e$, and on the holes, $\mathbf{F}_h$, as derived from these energies, are

$$F_{e\mu}=-\frac{\partial\varepsilon_{\rm p}^e}{\partial r_\mu}=-\frac{\partial\varepsilon_{1,\rm p}^e}{\partial u_{\nu\lambda}}\frac{\partial u_{\nu\lambda}}{\partial r_\mu}+eE_\mu$$
$$=-\Xi_e\frac{\partial u_{\nu\nu}}{\partial r_\mu}+eE_\mu\,,$$
$$F_{h\mu}=-\frac{\partial\varepsilon_{\rm p}^h}{\partial r_\mu}=-\frac{\partial\varepsilon_{1,\rm p}^h}{\partial u_{\nu\lambda}}\frac{\partial u_{\nu\lambda}}{\partial r_\mu}-eE_\mu \tag{2.5}$$
$$=\Xi_h\frac{\partial u_{\nu\nu}}{\partial r_\mu}-eE_\mu\,,$$

where $E_\mu=-\partial\phi/\partial r_\mu$ is the local electric field, and we have taken into account the fact that the Fermi seas are isotropic so that the deformation potentials can be written as

$$\frac{\partial\varepsilon_{1,\rm p}^e}{\partial u_{\mu\nu}}=\Xi_e\delta_{\mu\nu},\quad\frac{\partial\varepsilon_{1,\rm p}^h}{\partial u_{\mu\nu}}=-\Xi_h\delta_{\mu\nu}\,. \tag{2.6}$$

The sign of the hole deformation potential is such that the variation of the band gap with stress is proportional to $\Xi_e-\Xi_h$. We have neglected the momentum dependence in the last lines, because the deformation potentials are much larger than the Fermi energies themselves.

Similarly, we obtain the stress tensor for the ions,

$$\sigma_{\mu\nu}(\mathbf{r})=\frac{\delta E}{\delta u_{\mu\nu}}$$
$$=\frac{\delta E_{\rm ion}}{\delta u_{\mu\nu}}+\int d\Lambda\left[n_{\rm p}^e\frac{\partial\varepsilon_{\rm p}^e}{\partial u_{\mu\nu}}+n_{\rm p}^h\frac{\partial\varepsilon_{\rm p}^h}{\partial u_{\mu\nu}}\right]$$
$$=\sigma_{\mu\nu}^{\rm el}(\mathbf{r})+[n_e(\mathbf{r})\Xi_e-n_h(\mathbf{r})\Xi_h]\delta_{\mu\nu}\,, \tag{2.7}$$

where the momentum dependence has been neglected in the last line. The force acting on a unit volume of the lattice is given by

$$F_{i\mu}(\mathbf{r})=\frac{\partial\sigma_{\mu\nu}^{\rm el}}{\partial r_\nu}+\frac{\partial n_e}{\partial r_\mu}\Xi_e-\frac{\partial n_h}{\partial r_\mu}\Xi_h$$
$$+n_e\frac{\partial\Xi_e}{\partial u_{\nu\lambda}}\frac{\partial u_{\nu\lambda}}{\partial r_\mu}-n_h\frac{\partial\Xi_h}{\partial u_{\nu\lambda}}\frac{\partial u_{\nu\lambda}}{\partial r_\mu}\,. \tag{2.8}$$

The first term is the force without the electron-hole liquid, which determines the dispersion of a free sound wave in the solid. The sound and the third terms bring about attenuation of the sound, in which we are interested, as well as modify the sound velocity. The final two terms act only to modify the sound velocity, but produce a negligible effect since they contain factors, $n_{e\,(h)}$, which are much smaller than the density of ions (elastic constants are on the order of Ξ times the ion number density).

B. Kinetic equations for electrons and holes

We now calculate the response of the electrons and holes to the motion of the ions, by solving the linearized quantum kinetic equation[8] for each component,

$$[\hbar\omega-(\varepsilon_{\mathbf{p}+\hbar\mathbf{k}/2}^0-\varepsilon_{\mathbf{p}-\hbar\mathbf{k}/2}^0)]\delta n_{\rm p}(\mathbf{k},\omega)$$
$$+(n_{\mathbf{p}+\hbar\mathbf{k}/2}^0-n_{\mathbf{p}-\hbar\mathbf{k}/2}^0)\delta\varepsilon_{\rm p}(\mathbf{k},\omega)=iI[n_{\rm p'}^e,n_{\rm p'}^h]\,, \tag{2.9}$$

where $\delta n_{\rm p}$ is the shift of the distribution function from equilibrium, $n_{\rm p}^0$, and $\delta\varepsilon_{\rm p}$ is the shift of the single particle energy from $\varepsilon_{\rm p}^0$, the energy in the absence of strain and electric fields. The two kinetic equations for electrons and holes are of identical form, (2.9); generally, we omit the indices e or h indicating electrons or holes when the forms of the equations are similar.

The collision integral terms of (2.9) for electrons and holes, in general, couple the kinetic equations to each other and, if there are impurities, to the motion of the lattice. Interband collision times are much longer than intraband collision times since in realistic cases the phase space for the former is more limited; in addition, electron-impurity collisions can be neglected in the very pure samples usually used. We therefore assume that only the intraband collision time is relevant, and neglect all other collisions. The ionic motion then drives the electrons and holes simply through the dependence of $\varepsilon_1^{e\,(h)}$ on the strain field

$u_{\mu\nu}$. To make the problem tractable we adopt the relaxation-time approximation; then the collision integrals assume the simple form

$$I[n_{\mathbf{p}'}]=-\frac{\hbar}{\tau}[\delta n_{\mathbf{p}}(\mathbf{k},\omega)-\delta n_{\mathbf{p}}^{le}(\mathbf{k},\omega)]\ , \tag{2.10}$$

where $\delta n_{\mathbf{p}}^{le}$, the shift of the local equilibrium distribution, is given by

$$\delta n_{\mathbf{p}}^{le}(\mathbf{k},\omega)=-\frac{\partial n^0}{\partial\varepsilon}(\delta\mu+\mathbf{u}\cdot\mathbf{p})\ . \tag{2.11}$$

The shift of the chemical potential $\delta\mu$ reflects the change of the size of the Fermi sea, while the second term $\mathbf{u}\cdot\mathbf{p}$, where $\mathbf{u}$ is the drift velocity of the electrons (or holes), represents the shift of the center of the distribution.

Using (2.9)–(2.11) we obtain

$$\delta n_{\mathbf{p}}(\mathbf{k},\omega)=\frac{n^0_{\mathbf{p}-\hbar\mathbf{k}/2}-n^0_{\mathbf{p}+\hbar\mathbf{k}/2}}{\omega-\mathbf{v}\cdot\mathbf{k}+i/\tau}\frac{\delta\varepsilon_{\mathbf{p}}(k,\omega)}{\hbar} -\frac{i}{\tau}\frac{\partial n^0}{\partial\varepsilon}\frac{\delta\mu+\mathbf{u}\cdot\mathbf{p}}{\omega-\mathbf{v}\cdot\mathbf{k}+i/\tau}\ . \tag{2.12}$$

Equation (2.12) contains three quantities, $\delta\varepsilon_{\mathbf{p}}$, $\delta\mu$, and $\mathbf{u}$, which are related to the distribution function and ionic velocity in the following way. The shift of chemical potential $\delta\mu$ is related to the change of the number density by

$$\delta n=\int d\Lambda\,\delta n_{\mathbf{p}}=\frac{\partial n}{\partial\mu}\delta\mu=\frac{3n}{2\varepsilon_F}\delta\mu\ , \tag{2.13}$$

so that from (2.12) we have

$$\delta n=\frac{\delta\varepsilon}{\hbar}\int d\Lambda\frac{n^0_{\mathbf{p}-\hbar\mathbf{k}/2}-n^0_{\mathbf{p}+\hbar\mathbf{k}/2}}{\omega-\mathbf{v}\cdot\mathbf{k}+i/\tau} -\frac{i}{\tau}\int d\Lambda\frac{\partial n^0}{\partial\varepsilon}\frac{\delta\mu+\mathbf{u}\cdot\mathbf{p}}{\omega-\mathbf{v}\cdot\mathbf{k}+i/\tau}\ , \tag{2.14}$$

where the momentum dependence of $\delta\varepsilon_{\mathbf{p}}$ has been neglected. Then using (2.14), $\delta\mu$ can be written as

$$\delta\mu=L(\tilde{k},\tilde{\omega};\tilde{\tau})\delta\varepsilon+\frac{I_0(a)}{1-i\tilde{\omega}\tilde{\tau}}\delta\mu+\frac{2\varepsilon_F I_1(a)}{1-i\tilde{\omega}\tilde{\tau}}\tilde{\kappa}\ , \tag{2.15}$$

where the dimensionless functions L, I_0, and I_1 are written out explicitly in the Appendix, and the dimensionless variables are defined by

$$\begin{aligned}&\tilde{k}=k/k_F,\quad \tilde{\omega}=\hbar\omega/\varepsilon_F\ ,\\ &\tilde{\tau}=\varepsilon_F\tau/\hbar,\quad \tilde{\kappa}=u/v_F,\quad a=kv_F\tau/(1-i\omega\tau)\ .\end{aligned} \tag{2.16}$$

Thus

$$\delta\mu=\frac{(1-i\tilde{\omega}\tilde{\tau})L(\tilde{k},\tilde{\omega};\tilde{\tau})\delta\varepsilon+2\varepsilon_F I_1(a)\tilde{\kappa}}{1-i\tilde{\omega}\tilde{\tau}-I_0(a)}\ . \tag{2.17}$$

The electron or hole drift velocity $\mathbf{u}$ (or $\tilde{\mathbf{k}}$) is related to the corresponding current by $\mathbf{j}=n\mathbf{u}$. To determine $\mathbf{u}$ we write an expression for the current in a similar way,

$$\begin{aligned}\mathbf{j}=\int d\Lambda\,\delta n_{\mathbf{p}}\mathbf{v}&=\frac{\delta\varepsilon}{\hbar}\int d\Lambda\frac{n^0_{\mathbf{p}-\hbar\mathbf{k}/2}-n^0_{\mathbf{p}+\hbar\mathbf{k}/2}}{\omega-\mathbf{v}\cdot\mathbf{k}+i/\tau}\mathbf{v}-\frac{i}{\tau}\int d\Lambda\frac{\partial n^0}{\partial\varepsilon}\frac{\delta\mu+\mathbf{u}\cdot\mathbf{p}}{\omega-\mathbf{v}\cdot\mathbf{k}+i/\tau}\mathbf{v}\\ &=\left[\frac{3nv_F}{2\varepsilon_F}\left[J(\tilde{k},\tilde{\omega};\tilde{\tau})\delta\varepsilon+\frac{I_1(a)}{1-i\tilde{\omega}\tilde{\tau}}\delta\mu\right]+\frac{3I_2(a)}{1-i\tilde{\omega}\tilde{\tau}}\mathbf{j}\cdot\hat{\mathbf{k}}\right]\hat{\mathbf{k}}\ ,\end{aligned} \tag{2.18}$$

where J and I_2 are written explicitly in the Appendix. Substituting (2.17) into (2.18) we obtain

$$\mathbf{j}=\frac{\dfrac{3nv_F}{2\varepsilon_F}\left[J(\tilde{k},\tilde{\omega};\tilde{\tau})+\dfrac{L(\tilde{k},\tilde{\omega};\tilde{\tau})I_1(a)}{1-i\tilde{\omega}\tilde{\tau}-I_0(a)}\right]\delta\varepsilon}{1-\dfrac{3}{1-i\tilde{\omega}\tilde{\tau}}\{I_2(a)+I_1^2(a)/[1-i\tilde{\omega}\tilde{\tau}-I_0(a)]\}}\hat{\mathbf{k}}\ . \tag{2.19}$$

This expression has the same form for electrons and for holes, but with different parameters and scales, ε_F, v_F, and τ. The shifts of the single-particle energies $\delta\varepsilon$ are different for electrons and holes, and are given by (2.3); $\delta\varepsilon$ couples the motion of the electrons, holes, and ions through the deformation potential and the Coulomb interaction.

Since for a small oscillation of the lattice $\delta u_{\mu\mu}=-\mathbf{k}\cdot\mathbf{v}_i/\omega$, where $\mathbf{v}_i$ is the velocity of the ions, the change of the first terms of (2.3) for $\delta\varepsilon_{1,\mathbf{p}}$ can be expressed in terms of the deformation potentials and ionic velocity as

$$\delta\varepsilon_1^e=-\Xi_e\mathbf{k}\cdot\mathbf{v}_i/\omega,\quad \delta\varepsilon_1^h=\Xi_h\mathbf{k}\cdot\mathbf{v}_i/\omega\ . \tag{2.20}$$

The electrostatic potential $\phi(\mathbf{r})$ is given by (2.4) or, equivalently, by the Poisson equation

$$\nabla^2\phi(\mathbf{r})=-\frac{4\pi e}{\kappa}[n_e(\mathbf{r})-n_h(\mathbf{r})]\ . \tag{2.21}$$

Expressing the number densities of the electrons and the holes in terms of their currents, we may write

$$\begin{aligned}\phi(\mathbf{k},\omega)&=\frac{4\pi e^2}{\kappa k^2}[n_e(\mathbf{k},\omega)-n_h(\mathbf{k},\omega)]\\ &=\frac{4\pi e^2}{\kappa k^2}\frac{\mathbf{k}}{\omega}\cdot[\mathbf{j}_e(\mathbf{k},\omega)-\mathbf{j}_h(k,\omega)]\ ,\end{aligned} \tag{2.22}$$

and obtain

$$\delta\varepsilon^e=\frac{\mathbf{k}}{\omega}\cdot\left[\frac{4\pi e^2}{\kappa k^2}(\mathbf{j}_e-\mathbf{j}_h)-\Xi_e\mathbf{v}_i\right],\quad \delta\varepsilon^h=\frac{\mathbf{k}}{\omega}\cdot\left[\frac{4\pi e^2}{\kappa k^2}(\mathbf{j}_h-\mathbf{j}_e)+\Xi_h\mathbf{v}_i\right]\ . \tag{2.23}$$

The expressions for the current, (2.19) with (2.23), describe the motion of the electrons and the holes for a given motion of the ions $\mathbf{v}_i$. These equations become

$$\left[\frac{1}{P_e}-\frac{4\pi e^2}{\kappa k^2}\right]\mathbf{j}_e+\frac{4\pi e^2}{\kappa k^2}\mathbf{j}_h=-\Xi_e\mathbf{v}_i\ ,\quad \frac{4\pi e^2}{\kappa k^2}\mathbf{j}_e+\left[\frac{1}{P_h}-\frac{4\pi e^2}{\kappa k^2}\right]\mathbf{j}_h=\Xi_h\mathbf{v}_i\ , \tag{2.24}$$

where the polarizations P_e and P_h are given by

$$P_{e\,(h)}(\mathbf{k},\omega)=\frac{3n}{2\varepsilon_F}\frac{\dfrac{2\tilde{k}}{\tilde{\omega}}\left[J(\tilde{k},\tilde{\omega};\tau)+\dfrac{L(\tilde{k},\tilde{\omega};\tilde{\tau})I_1(a)}{1-i\tilde{\omega}\tilde{\tau}-I_0(a)}\right]}{1-\dfrac{3}{1-i\tilde{\omega}\tilde{\tau}}\{I_2(a)+I_1^2(a)/[1-i\tilde{\omega}\tilde{\tau}-I_0(a)]\}}\ , \tag{2.25}$$

with the corresponding electron or hole variables.

C. Motion of the lattice: Phonon self-energy

The motion of the ions is described by the acceleration equation

$$M_i n_i\frac{\partial\mathbf{v}_i}{\partial t}=\mathbf{F}_i\ , \tag{2.26}$$

where M_i and n_i are the mass and the number density of the ions, and the force $\mathbf{F}_i$ is given by (2.8). To determine the electron-hole–liquid contribution to the phonon self-energy we compute the extra force $\delta\mathbf{F}_i$ on the ions from the electron-hole liquid induced by the ionic motion. This extra force is determined by the second and third terms of (2.8), whose Fourier transform is

$$\begin{aligned}\delta\mathbf{F}_i&=i\mathbf{k}(\Xi_e\,\delta n_e-\Xi_h\,\delta n_h)\\&=i\frac{\mathbf{k}}{\omega}(\Xi_e\mathbf{k}\cdot\mathbf{j}_e-\Xi_h\mathbf{k}\cdot\mathbf{j}_h)\ .\end{aligned} \tag{2.27}$$

The final two terms of (2.9), as we have mentioned, give rise only to a small shift of the sound velocity, which we neglect here. Substituting the solution of (2.24) for $\mathbf{j}_e$ and $\mathbf{j}_h$, and expressing $\mathbf{v}_i$ in terms of the ionic displacement field, we obtain

$$\begin{aligned}\delta\mathbf{F}_i&=-k^2\frac{\Xi_e^2P_e+\Xi_h^2P_h-\dfrac{4\pi e^2}{\kappa k^2}(\Xi_e-\Xi_h)^2P_eP_h}{1-\dfrac{4\pi e^2}{\kappa k^2}(P_e+P_h)}\mathbf{u}\\&=-\Pi(k,\omega)M_in_i\mathbf{u}\ ,\end{aligned} \tag{2.28}$$

where $\Pi(k,\omega)$ is the phonon self-energy. The phonon dispersion relation is determined by the equation

$$\omega^2=c^2k^2+\Pi(k,\omega)\ , \tag{2.29}$$

where c is the sound velocity, $\mathbf{k}$ the phonon wave vector, and ω is its frequency; from (2.28), explicitly,

$$\Pi(k,\omega)=\frac{\Gamma_e^2P_e+\Gamma_h^2P_h-\dfrac{4\pi e^2}{\kappa k^2}(\Gamma_e-\Gamma_h)^2P_eP_h}{1-\dfrac{4\pi e^2}{\kappa k^2}(P_e+P_h)}\ , \tag{2.30}$$

where

$$\Gamma_e=\frac{k}{\sqrt{M_in_i}}\Xi_e,\quad \Gamma_h=\frac{k}{\sqrt{M_in_i}}\Xi_h \tag{2.31}$$

are the effective electron-phonon and hole-phonon matrix elements, and the polarizations P are given by (2.25).

The rate of energy attenuation, γ, of a sound wave is given in terms of Π by

$$\gamma(k)=-\frac{1}{\omega}\mathrm{Im}\Pi(k,\omega)\ , \tag{2.32}$$

evaluated at $\omega=\omega(k)$, the phonon dispersion relation.

D. Density of states, screening, and collisions

The formulas (2.30) and (2.25) are our principal results for the simplified band-structure model. The self-energy of the phonon, $\Pi(k,\omega)$, can be rewritten in the form

$$\begin{aligned}\Pi(k,\omega)&=\Gamma_e^2P_e+\Gamma_h^2P_h\\&\quad+(\Gamma_eP_e+\Gamma_hP_h)^2\frac{\dfrac{4\pi e^2}{\kappa k^2}}{1-\dfrac{4\pi e^2}{\kappa k^2}(P_e+P_h)}\ ,\end{aligned} \tag{2.33}$$

which brings out its relation to the random-phase-approximation (RPA) sum of polarization diagrams. Although this formula is similar to the RPA, the polarizations of the electrons and the holes, P_e and P_h, are modified here by intraband scattering.

Let us analyze (2.30) in several limits to understand its structure. When the Coulomb interaction is negligible, (2.30) or (2.33) is simply

$$\Pi(k,\omega)=\Gamma_e^2P_e+\Gamma_h^2P_h\ . \tag{2.34}$$

On the other hand, in the limit of strong Coulomb interactions Π becomes

$$\Pi(k,\omega)=(\Gamma_e-\Gamma_h)^2\frac{P_eP_h}{P_e+P_h}\ . \tag{2.35}$$

Let us first consider the case without electron collisions: $\tau\to\infty$. The polarizations are simply (see Appendix)

$$\begin{aligned}P(k,\omega;\tau\to\infty)&=\frac{3n}{2\varepsilon_F}\frac{2\tilde{k}}{\tilde{\omega}}J(\tilde{k},\tilde{\omega};\infty)\\&=\frac{3n}{2\varepsilon_F}L(\tilde{k},\tilde{\omega};\infty)\ ,\end{aligned} \tag{2.36}$$

which is simply the familiar Lindhard function. If there is no Coulomb interaction between electrons and holes, $e^2/\kappa \to 0$, the self-energy becomes (2.34). The contribution of the electrons and the holes are independent and additive. Its imaginary part is, as is well known, proportional to the square of the interaction matrix element, Γ, times the density of states energetically available, $(3n/2\varepsilon_F)\mathrm{Im}L$.

In Fig. 1(a) we display the phonon attenuation $\gamma(k)$ due to a single band, where we also illustrate the general effects of intraband collisions. In two-component systems $\gamma(k)$ is composed of two peaks. However, in our simple case these peaks are not separable since $k_F^e = k_F^h$, as shown in Fig. 1(b). $\gamma(k)$ increases linearly [see (A9)] as

$$\gamma(k) = \tfrac{3}{4}\pi \frac{n}{M_i n_i}\left[\frac{\Xi_e^2}{\varepsilon_F^e v_F^e} + \frac{\Xi_h^2}{\varepsilon_F^h v_F^h}\right] k \ , \tag{2.37}$$

and the separate components fall off at $k = 2k_F^e(1 - c/v_F^e)$ and $k = 2k_F^h(1 - c/v_F^h)$.

The Coulomb interaction among electrons and holes changes this feature. In the long-wavelength limit ($k \ll k_{\mathrm{TF}}$, where k_{TF} is the Thomas-Fermi screening wave number), the dynamical screening [described by the denominator in (2.30)] is always perfect and one is in the strong Coulomb interaction limit ($e^2/\kappa \to \infty$). In this limit, where Π is given by (2.35), the electrons and the holes move together and the reactions of each to the lattice are cooperative. The minus sign arises from the initial definition of the hole energy, which measures it opposite to the electron energy. The imaginary part of the self-energy is also proportional to k, and when the sound velocity is much smaller than the Fermi velocities, as is usually the case, $\gamma(k)$ can be written as

$$\gamma(k) = \tfrac{3}{4}\pi \frac{n}{M_i n_i}\left[\frac{\Xi_e - \Xi_h}{\varepsilon_F^e + \varepsilon_F^h}\right]^2 \left[\frac{\varepsilon_F^e}{v_F^e} + \frac{\varepsilon_F^h}{v_F^h}\right] k \ . \tag{2.38}$$

This can be either greater or smaller than the damping in the absence of Coulomb interactions, (2.37), depending on the values of the parameters.

The present situation differs from that in normal metals, since here the ions are neutral; Coulomb fields are produced only by the electrons and holes. Thus our expression (2.33) does not reduce in any limit to the usual expression[2,3] for ultrasonic attenuation in metals. However, in the limit $k \ll k_F$, $c \ll v_F$, $\omega\tau \ll 1$, we recover the hydrodynamic attenuation. In this case, as is shown in the Appendix,

$$\begin{aligned} L(\tilde{k} \to 0, \tilde{\omega}; \tilde{\tau}) &= -iaI_1(a) \ , \\ J(k \to 0, \tilde{\omega}; \tilde{\tau}) &= -iaI_2(a) \ , \end{aligned} \tag{2.39}$$

and (2.25) becomes

$$P(\tilde{k}, \tilde{\omega}; \tilde{\tau}) = -i\frac{k^2}{\omega}\frac{n\tau}{m}\frac{Y}{1 - Y} \ , \tag{2.40}$$

where

$$Y = \frac{3}{1 - i\omega\tau}\left[I_2(a) + \frac{I_1^2(a)}{1 - i\omega\tau - I_0(a)}\right] . \tag{2.41}$$

For $\omega\tau \ll 1$ and $kv_F\tau \ll 1$, (2.25) becomes

$$P(k,\omega) = -\frac{3n}{2\varepsilon_F}\left[\frac{1}{1 - 3(\omega/kv_F)^2} + \frac{4}{5}\frac{i\omega\tau}{[1 - 3(\omega/kv_F)^2]^2}\right] . \tag{2.42}$$

Then, were the Coulomb interaction negligible, one would have

$$\gamma(k) = \frac{6}{5}\frac{n}{M_i n_i}\left[\frac{\Xi_e^2}{[1 - 3(c/v_F^e)^2]^2}\frac{\tau_e}{\varepsilon_F^e} + \frac{\Xi_h^2}{[1 - 3(c/v_F^h)^2]^2}\frac{\tau_h}{\varepsilon_F^h}\right] k^2 \ , \tag{2.43}$$

which can be rewritten in the form

$$\gamma(k) = \frac{3}{M_i n_i}\left[\left[\frac{\Xi_e/\varepsilon_F^e}{1 - 3(c/v_F^e)^2}\right]^2 \eta_e + \left[\frac{\Xi_h/\varepsilon_F^h}{1 - 3(c/v_F^e)^2}\right]^2 \eta_h\right] k^2 \ , \tag{2.44}$$

where η_e and η_h are the viscosities of electron and hole gases:

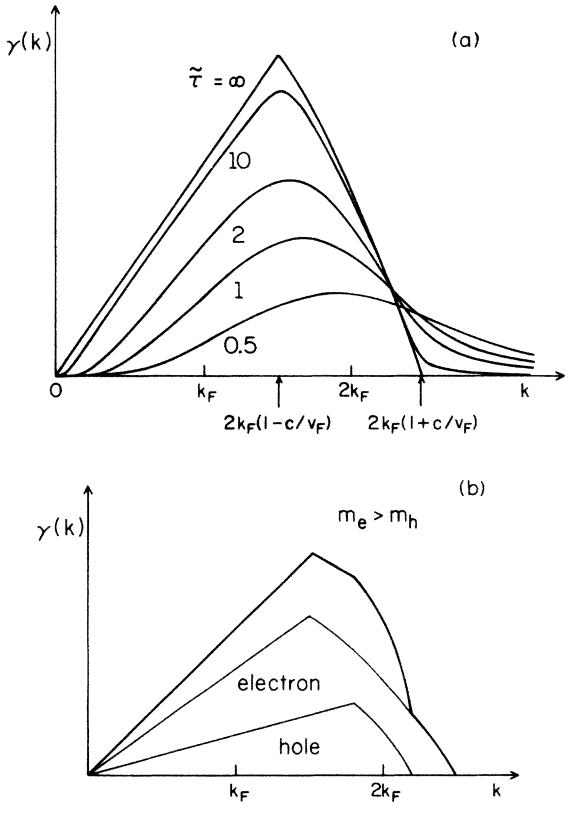

FIG. 1. (a) Attenuation of sound $\gamma(k)$ due to single component Fermi liquid. $\gamma(k)$ for a finite collision time τ is also illustrated. (b) $\gamma(k)$ in a two-component Fermi liquid in the absence of Coulomb interactions and collisions.

$$\eta_e=\tfrac{2}{5}\eta_e\varepsilon_F^e\tau_e,\quad \eta_h=\tfrac{2}{5}\eta_h\varepsilon_F^h\tau_h\ . \tag{2.45}$$

Usually $c\ll v_F$, and for a free Fermi gas $\Xi_e=\frac{2}{3}\varepsilon_F^e$ and $\Xi_h=-\frac{2}{3}\varepsilon_F^h$ (results by no means true for electron-hole liquids where $\varepsilon_F\ll|\Xi|$); in that case (2.44) is just the hydrodynamic attenuation of sound (with thermal conduction and second viscosity neglected),

$$\gamma(k)=\frac{4}{3}\frac{\eta}{\rho}k^2\ , \tag{2.46}$$

where ρ is the total mass density. The phonons would be dissipated by viscosity of the electron-hole liquid, with an enhanced coupling. Actually, the Coulomb interaction becomes dominant in the long-wavelength limit ($k\ll k_{\rm TF}$), and one should use (2.35), which gives (with $\eta_e=\eta_h=\eta$)

$$\gamma(k)=\frac{6}{5}\frac{n}{M_i n_i}\left[\frac{\Xi_e-\Xi_h}{[1-3(c/v_F^e)^2]\varepsilon_F^e+[1-3(c/v_F^h)^2]\varepsilon_F^h}\right]^2(\varepsilon_F^e\tau_e+\varepsilon_F^h\tau_h)k^2\ . \tag{2.47}$$

Generally, the effects of the electrons and holes are no longer separable. However, for $c\ll v_F$ and with Ξ_i given by the free-gas values, (2.47) reduces exactly to (2.46). When the wavelength of sound is shorter than the mean free path, $kv_F\tau\gg1$, and $kv_F\gg\omega$, (2.41) becomes

$$P(k,\omega)=-\frac{3n}{2\varepsilon_F}\left[1+i\frac{\pi}{2}\frac{\omega}{kv_F}\right], \tag{2.48}$$

which gives the same attenuation as (2.37).

Although we have examined several limiting cases to elucidate (2.30), in order to see its full behavior it is necessary to resort to numerical calculations, which are done in the next section for more realistic models.

III. MULTIVALLEY SYSTEMS

In real electron-hole liquids in semiconductors such as Ge and Si the band structure is not simple; there are several valleys which are very anisotropic, and the bands can be degenerate. In recent experiments, Dietsche, Kirch, and Wolfe[1] measured the absorption of monochromatic phonons by an electron-hole liquid over the frequency range $\omega/2\pi=150$–500 GHz and found that they could not fit the overall magnitude of their results within existing theory[9] using independently determined deformation potentials, suggesting a possibly important role of screening. We focus here on applying the theory developed in the preceding section for longitudinal acoustic sound in Ge propagating along the ⟨111⟩ direction in order to understand these effects. The good symmetry of the ⟨111⟩ direction keeps the current in this direction and allows us to use a simple extension of the theory. We also carry out a similar calculation for sound propagation in the ⟨100⟩ direction of Si.

We develop first the theory for electron-hole liquids in Ge and calculate the phonon self-energy in subsection A. The results of numerical calculations are presented in subsection B, and are compared with experiment. Our calculations indicate the importance of electron-electron and hole-hole collisions, rather than screening, in bringing theory and experiment into agreement.

A. Calculation of phonon self-energy

The electron valleys in Ge are spheroids with their symmetry axes along the [111] direction and the three equivalent directions: $[1\bar1\bar1]$, $[\bar1\,1\bar1]$, and $[\bar1\bar1\,1]$. The electron mass of this direction, $m_{||}$, is much larger than that of the orthogonal directions, $m_\perp$, and the Fermi momentum of this direction, $p_F^{||}$, is much larger than that of the orthogonal direction, $p_F^\perp$. (All relevant numbers are summarized in Table I.) The two hole Fermi seas are at the center of the Brillouin zone and are degenerate, with a very small mass. We approximate the hole Fermi seas by a single spherical one, which has the same number of holes and the same Fermi energy.

For sound propagation along [111], we distinguish electrons in the [111] valley from those in the other three valleys, since their interaction with the lattice and their response to an electric field are different. The shift of the single-electron energy of the lth band due to deformation of the lattice is usually written as[10]

$$\delta\varepsilon^l=(\Xi_d+\tfrac{1}{3}\Xi_u)u_{\lambda\lambda}+\Xi_u(\eta_\mu^l u_{\mu\nu}\eta_\nu^l-\tfrac{1}{3}u_{\lambda\lambda})\ , \tag{3.1}$$

where η_μ^l is the unit vector along the center of the valley. We choose the direction of sound propagation [111] as the z axis; then the deformation potential of the [111] valley, Ξ_1, and that of the other three valleys, Ξ_3, are given by

$$\Xi_1=\frac{\partial\varepsilon_1}{\partial u_{zz}}=\Xi_d+\Xi_u\ ,\qquad \Xi_3=\frac{\partial\varepsilon_3}{\partial u_{zz}}=\Xi_d+\tfrac{1}{9}\Xi_u\ . \tag{3.2}$$

Therefore for longitudinal sound in the [111] direction we have three different deformation potentials: Ξ_1,Ξ_3 for the electrons, and Ξ_h for the holes.

There are now five kinetic equations for each Fermi sea, three of them similar. The one for the holes is the same as that in Sec. II, and the calculation of their response is also the same as we have done in Sec. II. However, the calculation for the electrons is different because of the ellipsoidal Fermi sea. The ground-state electron Fermi sea Ω_0 is given (with the z axis along the symmetry axis of the ellipsoid) by

$$\frac{1}{2m_\perp}(p_x^2+p_y^2)+\frac{1}{2m_{||}}p_z^2\le\varepsilon_F^e\ . \tag{3.3}$$

If we scale the momentum by the Fermi momentum of each direction and the energy by the Fermi energy, the scaled Fermi sea $\tilde\Omega_0$ is

$$\tilde p_x^2+\tilde p_y^2+\tilde p_z^2\le1\ , \tag{3.4}$$

where

$$\tilde{\mathbf{p}}=(p_x/p_F^\perp,\,p_y/p_F^\perp,\,p_z/p_F^{||})\ .$$

TABLE I. List of parameters used for Ge.

Ion mass	M_i	1.21×10^{-22} g
Ion number density	n_i	4.42×10^{22} cm^{-3}
Sound velocity	c	5.6×10^{5} cm sec^{-1}
Dielectric constant	κ	16
Pair number density	n	2.3×10^{17} cm^{-3}
Electron Fermi energy	ε_F^e	4.05×10^{-15} erg (2.53 meV)
Electron effective mass	$m_\perp$	7.47×10^{-29} g ($0.082\,m_{\text{electron}}$)
	$m_{\|\|}$	1.42×10^{-27} g ($1.56\,m_{\text{electron}}$)
Electron Fermi wave number	$k_F^\perp=(2m_\perp\varepsilon_F^e)^{1/2}/\hbar$	7.41×10^{5} cm^{-1}
	$k_F^{\|\|}=(2m_{\|\|}\varepsilon_F^e)^{1/2}/\hbar$	3.23×10^{6} cm^{-1}
	k_F^3	7.83×10^{5} cm^{-1}
Electron Fermi velocity	$v_F^\perp=(2\varepsilon_F^e/m_\perp)^{1/2}$	1.04×10^{7} cm sec^{-1}
	$v_F^{\|\|}=(2\varepsilon_F^e/m_{\|\|})^{1/2}$	2.39×10^{6} cm sec^{-1}
	v_F^3	9.86×10^{6} cm sec^{-1}
Hole Fermi energy	ε_F^h	6.2×10^{-15} erg (3.9 meV)
Hole effective mass	$m_h=(\hbar k_F^h)^2/2\varepsilon_F^h$	3.2×10^{-28} g ($0.35\,m_{\text{electron}}$)
Hole Fermi wave number	$k_F^h=(3\pi^2n)^{1/3}$	1.9×10^{6} cm^{-1}
Hole Fermi velocity	v_F^h	6.2×10^{6} cm sec^{-1}
Electron deformation potential[a]	$\Xi_1=\Xi_d+\Xi_u$	1.12×10^{-11} erg, $\Xi_d=-12.3$ eV
	$\Xi_3=\Xi_d+\frac{1}{9}\Xi_u$	-1.62×10^{-11} erg, $\Xi_u=19.3$ eV
Hole deformation potential[b]	Ξ_h	-4.8×10^{-12} erg (-3 eV)
Thomas-Fermi wave number (for holes)	$k_{\text{TF}}^h=(6\pi e^2n/\kappa\varepsilon_F^h)^{1/2}$	3.2×10^{6} cm^{-1}

[a]Reference 11.
[b]Reference 12.

The local equilibrium Fermi sea with wave number shift $\boldsymbol{\kappa}(\mathbf{r},t)$ and chemical potential shift $\delta\mu(\mathbf{r},t)$ is given by

$$\frac{1}{2m_\perp}(p_x-\hbar\kappa_x)^2+\frac{1}{2m_\perp}(p_y-\hbar\kappa_y)^2+\frac{1}{2m_{||}}(p_z-\hbar\kappa_z)^2\le\varepsilon_F^e+\delta\mu\ , \tag{3.5}$$

or in the scaled space

$$(\tilde p_x-\tilde\kappa_x)^2+(\tilde p_y-\tilde\kappa_y)^2+(\tilde p_z-\tilde\kappa_z)^2\le1+\delta\tilde\mu\ , \tag{3.6}$$

where

$$\tilde{\boldsymbol{\kappa}}=(\tilde\kappa_x/k_F^\perp,\tilde\kappa_y/k_F^\perp,\tilde\kappa_z/k_F^{||})$$

is the shift of the scaled Fermi sphere and $\delta\tilde\mu=\delta\mu/\varepsilon_F^e$. For small shifts the change of number density and the current are given by

$$n+\delta n=\int d\Lambda\, n^{le}=n(1+\tfrac{3}{2}\delta\tilde\mu)\ , \tag{3.7}$$

$$\mathbf{j}=\int d\Lambda\, n^{le}\mathbf{v}=n(v_F^\perp\tilde\kappa_x,v_F^\perp\tilde\kappa_y,v_F^{||}\tilde\kappa_z)=n\mathbf{u}\ . \tag{3.8}$$

The last equality of (3.8) defines the drift velocity $\mathbf{u}$.

When $\mathbf{k}$ is parallel to the symmetry axis (z axis), as is the case for the [111] valley, the current is also in this direction. Using the dimensionless functions given in the Appendix, we can calculate the change of the number density and the current in a similar way as we have done in Sec. II. The magnitude of the current j_1 is [cf. (2.18)]

$$j_1=\frac{3n_1}{2\varepsilon_F^e}\left[\left[J(\tilde k_1,\tilde\omega_1;\tilde\tau_1)+\frac{L(\tilde k_1,\tilde\omega_1;\tilde\tau_1)I_1(a_1)}{1-i\tilde\omega_1\tilde\tau_1-I_0(a_1)}\right]\delta\varepsilon^1+\frac{1}{1-i\tilde\omega_1\tilde\tau_1}\left[I_2(a_1)+\frac{I_1^2(a_1)}{1-i\tilde\omega_1\tilde\tau_1-I_0(a_1)}\right]2\varepsilon_F^e\tilde\kappa_1\right]v_F^{||}\ , \tag{3.9}$$

where we denote all quantities corresponding this valley by the suffix 1:

$$\tilde k_1=\frac{k}{k_F^{||}},\quad\tilde\omega_1=\frac{\hbar\omega}{\varepsilon_F^e},\quad\tilde\tau_1=\frac{\varepsilon_F^e\tau_e}{\hbar},\quad a_1=\frac{2\tilde k_1\tilde\tau_1}{1-i\tilde\omega_1\tilde\tau_1},\quad\tilde\kappa_1=\frac{\kappa_1}{k_F^{||}}=\frac{j_1}{n_1v_F^{||}}\ . \tag{3.10}$$

This current for the other three electron valleys is not parallel to $\mathbf{k}$ (see Fig. 2). However, by symmetry the transverse components of the three valleys cancel out and the net current is parallel to $\mathbf{k}$; therefore the force acting on the electrons in these valleys is also in the [111] direction. We expect that the shift of momentum of these Fermi seas, $\hbar\kappa_3$ (all quantities of these valleys are denoted by suffix 3), is parallel to $\mathbf{k}$, since it is due to the force $\mathbf{F}_3$ which is parallel to $\mathbf{k}$. Therefore using (A3), (A17), and (A18) we obtain an equation similar to (2.17). With the help of this equation, together with (A6), (A19), and (A20), we find that the current of each of these valleys is

$$\mathbf{j}=\frac{3n_1}{2\varepsilon_F^e}\left[\left[J(\tilde{k}_3,\tilde{\omega}_3;\tilde{\tau}_3)+\frac{L(\tilde{k}_3,\tilde{\omega}_3;\tilde{\tau}_3)I_1(a_3)}{1-i\tilde{\omega}_3\tilde{\tau}_3-I_0(a_3)}\right]\delta\varepsilon^3+\frac{1}{1-i\tilde{\omega}_3\tilde{\tau}_3}\left[I_2(a_3)+\frac{I_1^2(a_3)}{1-i\tilde{\omega}_3\tilde{\tau}_3-I_0(a_3)}\right]2\varepsilon_F^e\tilde{\kappa}_3\right]\left[v_F^{\perp}\frac{\tilde{k}_{3x}}{\tilde{k}_3},0,v_F^{\parallel}\frac{\tilde{k}_{3z}}{\tilde{k}_3}\right], \tag{3.11}$$

where we have chosen the x axis as in Fig. 2, so that $\tilde{\mathbf{k}}_3=(k_x/k_F^{\perp},0,k_z/k_F^{\parallel})$ and

$$\begin{aligned}&\tilde{k}_3=|\tilde{\mathbf{k}}_3|=\frac{k}{k_F^{\parallel}}\left[\cos^2\alpha+\frac{m_{\parallel}}{m_{\perp}}\sin^2\alpha\right]^{1/2}\equiv\frac{k}{k_F^3},\\&\tilde{\omega}_3=\frac{\hbar\omega}{\varepsilon_F^e}\ (=\tilde{\omega}_1),\quad\tilde{\tau}_3=\frac{\varepsilon_F^e\tau_e}{\hbar}\ (=\tilde{\tau}_1),\quad a_3=\frac{2\tilde{k}_3\tilde{\tau}_3}{1-i\tilde{\omega}\tilde{\tau}_3},\quad\tilde{\kappa}_3=|\tilde{\boldsymbol{\kappa}}_3|=\frac{\kappa_3}{k_F^3}.\end{aligned} \tag{3.12}$$

The direction of $\tilde{\mathbf{k}}_3$ is given by

$$(\tilde{k}_{3x},\tilde{k}_{3y},\tilde{k}_{3z})/\tilde{k}_3=\left[\frac{\sin\alpha}{\sqrt{m_{\perp}}},0,\frac{\cos\alpha}{\sqrt{m_{\parallel}}}\right]\Big/\left[\frac{\cos^2\alpha}{m_{\parallel}}+\frac{\sin^2\alpha}{m_{\perp}}\right]^{1/2}, \tag{3.13}$$

where α is the angle between $\mathbf{k}$ and the z axis, and $\cos\alpha=-\frac{1}{3}$. From (3.11) and (3.13) the direction of the current is given by

$$(j_x,j_y,j_z)/j=\left[\frac{\sin\alpha}{m_{\perp}},0,\frac{\cos\alpha}{m_{\parallel}}\right]\Big/\left[\frac{\cos^2\alpha}{m_{\parallel}^2}+\frac{\sin^2\alpha}{m_{\perp}^2}\right]^{1/2}\equiv(\sin\beta,0,\cos\beta). \tag{3.14}$$

The magnitude of the net current due to the three valleys, j_3, is

$$j_3=3\mathbf{j}\cdot\frac{\mathbf{k}}{k}, \tag{3.15}$$

which is related to $\tilde{\kappa}_3$ by

$$\begin{aligned}\tilde{\kappa}_3&=\frac{j}{n_1v_F^{\parallel}}\left[\cos^2\beta+\frac{m_{\perp}}{m_{\parallel}}\sin^2\beta\right]^{1/2}\\&=\frac{1}{n_1v_F^{\parallel}}\frac{j_3}{3\cos(\beta-\alpha)}\left[\cos^2\beta+\frac{m_{\perp}}{m_{\parallel}}\sin^2\beta\right]^{1/2}\\&=\frac{j_3}{n_3v_F^{\parallel}}\left[\cos^2\alpha+\frac{m_{\parallel}}{m_{\perp}}\sin^2\alpha\right]^{-1/2},\end{aligned} \tag{3.16}$$

where n_3 $(=3n_1)$ is the number density of the three valleys combined. Then,

$$j_3=\frac{\frac{3n_3}{2\varepsilon_F^e}v_{\parallel}\left[\cos^2\alpha+\frac{m_{\parallel}}{m_{\perp}}\sin^2\alpha\right]^{1/2}\left[J+\frac{LI_1}{1-i\tilde{\omega}_3\tilde{\tau}_3-I_0}\right]}{1-[3/(1-i\tilde{\omega}_3\tilde{\tau}_3)][I_2+I_1^2/(1-i\tilde{\omega}_3\tilde{\tau}_3-I_0)]}. \tag{3.17}$$

The changes of the single-particle energies, corresponding to (2.23), are

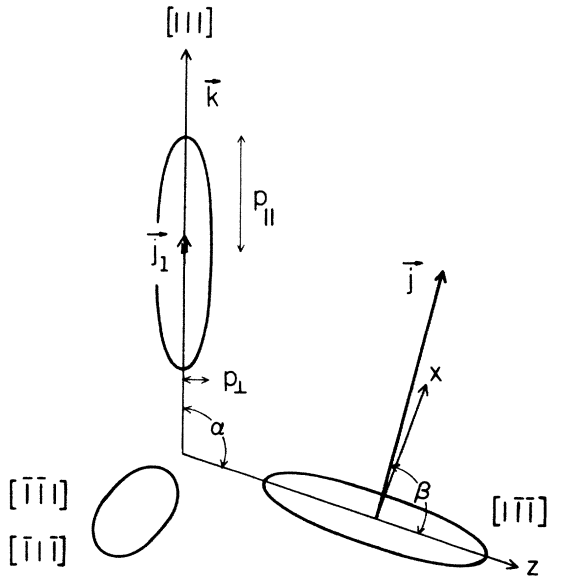

FIG. 2. Spheroidal electron Fermi seas in Ge. Currents due to the Fermi seas other than for the [111] direction are not parallel to $\mathbf{k}$ (along [111]).

$$\delta\varepsilon^1=\frac{k}{\omega}\left[\frac{4\pi e^2}{\kappa k^2}(j_1+j_3-j_h)-\Xi_1 v_i\right],$$

$$\delta\varepsilon^3=\frac{k}{\omega}\left[\frac{4\pi e^2}{\kappa k^2}(j_1+j_3-j_h)-\Xi_3 v_i\right], \tag{3.18}$$

$$\delta\varepsilon^h=\frac{k}{\omega}\left[\frac{4\pi e^2}{\kappa k^2}(j_h-j_1-j_3)+\Xi_h v_i\right].$$

Substituting these equations into (3.9), (3.17), and the corresponding equation for the holes, and bearing in mind the following relations,

$$\frac{k}{\omega}v_F^{\parallel}=\frac{2\tilde{k}_1}{\tilde{\omega}_1},\quad \frac{k}{\omega}v_F^{h}=\frac{2k_{\hbar}}{\tilde{\omega}_h}$$

$$\frac{k}{\omega}v_F^{\parallel}\left[\cos^2\alpha+\frac{m_{\parallel}}{m_{\perp}}\sin^2\alpha\right]^{1/2}\left[\equiv\frac{k}{\omega}v_F^{3}\right]=\frac{2\tilde{k}_3}{\tilde{\omega}_3}, \tag{3.19}$$

we obtain the simple system of equations

$$\begin{aligned}
&\frac{1}{P_1}j_1-\frac{4\pi e^2}{\kappa k^2}(j_1+j_3-j_h)=-\Xi_1 v_i,\\
&\frac{1}{P_3}j_3-\frac{4\pi e^2}{\kappa k^2}(j_1+j_3-j_h)=-\Xi_3 v_i,\\
&\frac{4\pi e^2}{\kappa k^2}(j_1+j_3-j_h)+\frac{1}{P_h}j_h=\Xi_h v_i,
\end{aligned} \tag{3.20}$$

where

$$P_j(k,\omega)=\frac{3n_j}{2\varepsilon_F^i}\frac{\frac{2\tilde{k}_j}{\tilde{\omega}_j}\{J(\tilde{k}_j,\tilde{\omega}_j;\tilde{\tau}_j)+L(\tilde{k}_j,\tilde{\omega}_j;\tilde{\tau}_j)I_1(a_j)/[1-i\tilde{\omega}_j\tilde{\tau}_j-I_0(a_j)]\}}{1-\frac{3}{1-i\tilde{\omega}_j\tilde{\tau}_j}\{I_2(a_j)+I_1^2(a_j)/[1-i\tilde{\omega}_j\tilde{\tau}_j-I_0(a_j)]\}}, \tag{3.21}$$

and $j=(1,3,h)$.

Following the same procedure as in Sec. II, we obtain the self-energy of the phonon,

$$\Pi(k,\omega)=\left[\Gamma_1^2P_1+\Gamma_3^2P_3+\Gamma_h^2P_h-\frac{4\pi e^2}{\kappa k^2}[(\Gamma_1-\Gamma_3)^2P_1P_3+(\Gamma_3-\Gamma_h)^2P_3P_h+(\Gamma_h-\Gamma_1)^2P_hP_1]\right]\Big/\left[1-\frac{4\pi e^2}{\kappa k^2}(P_1+P_3+P_h)\right], \tag{3.22}$$

where

$$\Gamma_1=\frac{k}{\sqrt{M_in_i}}\Xi_1,\quad \Gamma_3=\frac{k}{\sqrt{M_in_i}}\Xi_3,\quad \Gamma_h=\frac{k}{\sqrt{M_in_i}}\Xi_h. \tag{3.23}$$

Note that (3.22) can be rewritten as

$$\Pi(k,\omega)=\Gamma_1^2P_1+\Gamma_3^2P_3+\Gamma_h^2P_h+\frac{(\Gamma_1P_1+\Gamma_3P_3+\Gamma_hP_h)^2\frac{4\pi e^2}{\kappa k^2}}{1-\frac{4\pi e^2}{\kappa k^2}(P_1+P_3+P_h)}. \tag{3.24}$$

B. Results of numerical calculation and comparison with experiment

In this section we present the results of numerical calculations of the sound attenuation γ, from Eq. (3.22). The parameters used are given in Table I, and we assume zero temperature. Figure 3 shows the result for $\tau=\infty$, i.e., no electron (hole) relaxation, $\kappa=\infty$, no screening, $\kappa=1$, and $\kappa=16$. We see three peaks, due—in order of decreasing frequency—to [111] electrons, the holes, and the electrons in the other valleys. In the case of $\kappa=\infty$ the attenuation is just the sum of the three separate contribu-

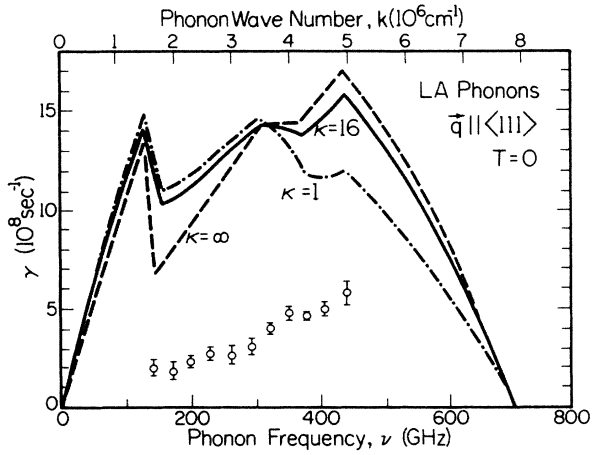

FIG. 3. Attenuation of longitudinal sound as function of frequency $\nu=\omega/2\pi$, along the ⟨111⟩ direction, in a Ge electron-hole liquid, $\gamma(k)$, in the absence of electron (hole) relaxation ($\tau=\infty$), for different strengths of the Coulomb interaction: $\kappa=\infty$, $\kappa=16$, and $\kappa=1$. At long wavelengths, $k\ll k_{\rm TF}$, the screening is always perfect. The experimental data (Ref. 1) are also shown. The absolute normalization of the experimental points is uncertain to within + 100%, −50%.

tions, and is what one could derive from simple perturbation theory. The initial slope is determined by

$$\gamma(k)=\frac{3\pi n}{4M_i n_i}\left[\frac{\Xi_1^2}{4\varepsilon_F^e v_F^{\parallel}}+\frac{3\Xi_3^2}{4\varepsilon_F^e v_F^3}+\frac{\Xi_h^2}{\varepsilon_F^h v_F^h}\right]k\ , \tag{3.25}$$

where n is the number density of electron-hole pairs.

The curves for $\tau=\infty$ and $\kappa=16$ and $\kappa=1$ show the effect of screening. For small k ($\ll k_{\rm TF}$) screening (terms $\propto k^{-2}$) always dominates, and to lowest order in c/v_F the initial slope is determined by

$$\gamma(k)=\tfrac{3}{16}\pi\frac{n}{M_i n_i}\left\{\left[\frac{\Xi_1-\Xi_3}{\varepsilon_F^e+\varepsilon_F^h}\right]^2\left[\left(\frac{9}{16}\frac{1}{v_F^{\parallel}}+\frac{3}{16}\frac{1}{v_F^3}\right)\frac{(\varepsilon_F^h)^2}{\varepsilon_F^e}+\frac{3}{4}\left(\frac{1}{v_F^{\parallel}}+\frac{1}{v_F^3}-\frac{1}{v_F^h}\right)\varepsilon_F^h\right]\right.$$
$$+\left[\frac{\Xi_3-\Xi_h}{\varepsilon_F^e+\varepsilon_F^h}\right]^2\left[\frac{3}{v_F^3}\varepsilon_F^e+\left(\frac{3}{v_F^h}+\frac{3}{4}\frac{1}{v_F^3}-\frac{3}{4}\frac{1}{v_F^{\parallel}}\right)\varepsilon_F^h\right]$$
$$\left.+\left[\frac{\Xi_h-\Xi_1}{\varepsilon_F^e+\varepsilon_F^h}\right]^2\left[\frac{1}{v_F^{\parallel}}\varepsilon_F^e+\left(\frac{1}{v_F^h}+\frac{3}{4}\frac{1}{v_F^{\parallel}}-\frac{3}{4}\frac{1}{v_F^3}\right)\varepsilon_F^h\right]\right\}k\ . \tag{3.26}$$

This slope is about 1.2 times larger than (3.25). In this case screening increases the damping in the long-wavelength region. At short wavelengths, although the effect of screening is not very simple, it decreases the damping. For a large dielectric constant, screening does not change the damping very much. (These conclusions, based on the parameters in Table I, depend, of course, on the values of these parameters.)

In Fig. 4 the effects of the electron (hole) relaxation time are shown. For illustration we take $\tau_e=\tau_h$ ($\equiv\tau$), and $\kappa=16$. Finite relaxation times round the shape, and, for $\tau\lesssim 10^{-12}$ sec, decrease the damping considerably. At long wavelengths [$k\ll k_{\rm TF}, k_F, (v_F\tau)^{-1}$] the damping is proportional to $k^2\tau$ and given (for $c\ll v_F$) by [cf. (2.46)]

$$\gamma(k)=\frac{3}{10}\frac{n}{M_i n_i}\left[\frac{3}{4}\frac{\varepsilon_F^h}{\varepsilon_F^e}(\Xi_1-\Xi_3)^2+3(\Xi_3-\Xi_h)^2\right.$$
$$\left.+(\Xi_h-\Xi_1)^2\right]\frac{\tau}{\varepsilon_F^e+\varepsilon_F^h}k^2\ . \tag{3.27}$$

In the same figure we show the experimental results of Dietsche, Kirch, and Wolfe.[1] In their paper they compared their results with the value expected for [111] electrons with screened deformation potentials calculated by Markiewicz.[13] In fact, the results in the strong Coulomb interaction limit, (2.38) and (3.26), can be expressed in the form of (2.37) and (3.26) with adequate screened deformation potentials. However, as they noticed, one cannot use these screened deformation potentials for large k. The observed damping was about one-tenth of the calculated value,[1] and one-third of the value expected for [111] electrons without electron-electron Coulomb interactions (the curve for $\kappa=\infty$ in Fig. 3). Our calculation (the curves for $\kappa=16$ and $\kappa=1$ in Fig. 3) shows that the effect of screening is not very large. Therefore the significant decrease of the damping is probably due to the relaxation of the electrons and holes (see Fig. 4). Although there is great experimental difficulty in determining the absolute magnitude of the damping (it is uncertain to a factor 2), comparison of our calculation to the data suggests that the relaxation time τ is about 10^{-13} sec. Except at short wavelengths, the general trend of the k dependence is similar in both the experimental and calculated curves. Possible reasons for the discrepancies between theory and experiment are the ambiguity of the values of the deformation potentials and the limitation of the single-relaxation-time approximation of the collision integrals.

We also present the result of a similar calculation for longitudinal-acoustic sound in Si propagating along the ⟨100⟩ direction. In Si, the electron Fermi seas, six in number, are spheroids with symmetry axes in the [100] and equivalent directions. The calculation is simpler than

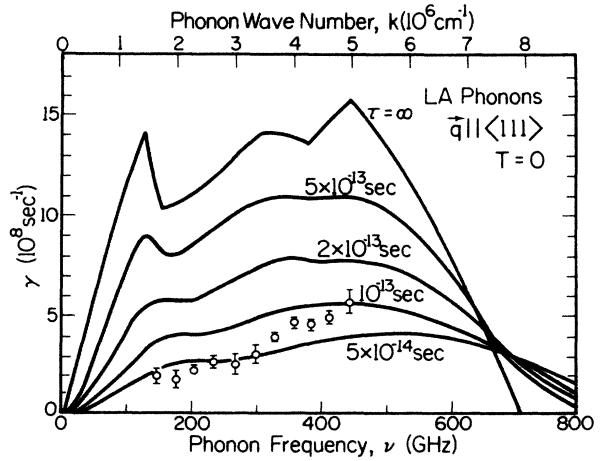

FIG. 4. Attenuation of longitudinal sound along the ⟨111⟩ direction in a Ge electron-hole liquid, $\gamma(k)$, with electron (hole) relaxation. The data points are the same as in Fig. 3.

TABLE II. List of parameters used for Si.

M_i	4.66×10^{-23} g	
n_i	5.00×10^{22} cm^{-3}	
c	8.5×10^{5} cm sec^{-1}	
κ	12	
n	3.3×10^{18} cm^{-3}	
ε_F^e	1.25×10^{-14} erg	
$m_\perp$	1.73×10^{-28} g ($0.19m_{\text{electron}}$)	
$m_\parallel$	8.93×10^{-28} g ($0.98m_{\text{electron}}$)	
$k_F^\perp$	1.98×10^{6} cm^{-1}	
$k_F^\parallel$	4.50×10^{6} cm^{-1}	
$v_F^\perp$	1.20×10^{7} cm sec^{-1}	
$v_F^\parallel$	5.29×10^{6} cm sec^{-1}	
ε_F^h	2.30×10^{-14} erg	
m_h	5.08×10^{-28} g ($0.56m_{\text{electron}}$)	
k_F^h	4.61×10^{6} cm^{-1}	
v_F^h	9.52×10^{6} cm sec^{-1}	
Ξ_1[a]	4.8×10^{-12} erg	$\Xi_d=-6.0$ eV
Ξ_2[b]	-9.6×10^{-12} erg	$\Xi_u=9.0$ eV
Ξ_h	-4.8×10^{-12} erg	
k_{TF}^h	7.2×10^{6} cm^{-1}	

[a]The deformation potential (Ref. 11) for electrons in [100] and [$\bar{1}$00] valleys: $\Xi_1=\Xi_d+\Xi_u$.
[b]The deformation potential (Ref. 12) for electrons in the other valleys: $\Xi_2=\Xi_d$.

in Ge since in this case $\mathbf{k}$ is along a principal axis of each spheroid. The parameters used are given in Table II, and the result in Fig. 5 (see Ref. 12). In this case the frequency scale is larger since the electron-hole liquid in Si is denser. Peaks due to electrons in the [100] direction and holes are not separated. There is at present no experimental information available for the attenuation in Si.

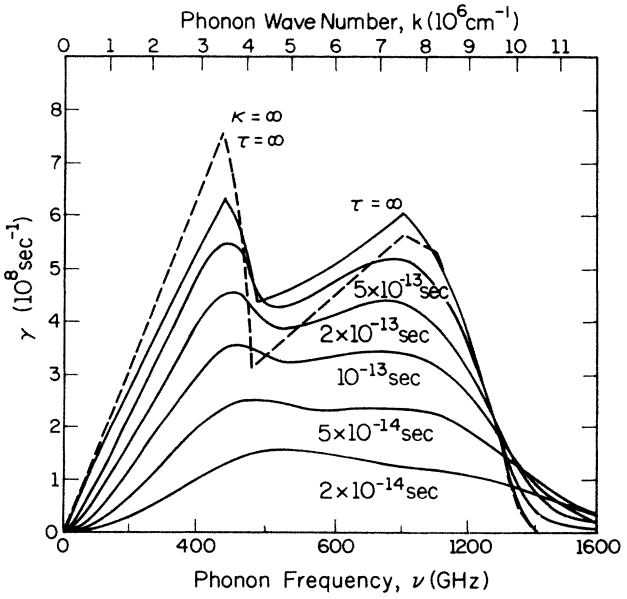

FIG. 5. Attenuation, in a Si electron-hole liquid, of longitudinal acoustic sound propagating along the [100] direction.

IV. DISCUSSION

Our principal result, Eq. (3.22) with (3.21), or in the idealized case (2.30), for the phonon self-energy, contains a unified description of phonon attenuation at all wave numbers [as well as the frequency shift, when the final two terms of Eq. (2.8) are included] due to the coupling of the phonon to the electron-hole liquid. The result is valid at finite as well as zero temperature, and includes density-of-states effects, Coulomb interactions and their screening, and intraband scattering processes as described by a relaxation time. Detailed numerical calculations for Ge and Si show that the effect of Coulomb interactions is relatively small in both cases, and that a short relaxation time $\tau\lesssim10^{-12}$ sec decreases the attenuation considerably, thus removing the serious discrepancy between the experiment[1] on Ge and the simple perturbation result (the $\kappa=\infty$ curve in Fig. 3) neglecting Coulomb interactions and relaxation processes.

Comparison of theory and experiment in Ge suggests that τ is of order 10^{-13} sec. In view of the experimental uncertainty in the absolute normalization of the data, and the use of the single-relaxation-time approximation, it is not possible to determine this τ more precisely at present. The ultrasonic experiments are, in fact, in the regime where k is comparable to k_F. Typically, k is comparable to or larger than the k_F (in the direction of $\hat{\mathbf{k}}$) of the valleys that contribute dominantly to the damping. For example, at $k=5\times10^{6}$ cm^{-1}, where valley 1 provides the peak (Fig. 4, for $\tau=\infty$), one has $k_F^\parallel=3.23\times10^{6}$ cm^{-1}. Since the effective τ should depend strongly on k/k_F, as well as on $\hbar\omega/\varepsilon_F$ (which for the electrons equals unity at $\omega=3.84\times10^{12}$ sec^{-1}), we expect the effective τ to vary across the range of phonon wave vectors shown in Fig. 4. Calculation of the effective $\tau(\mathbf{k},\omega)$ through a more careful treatment of the collision integral in the kinetic equations, beyond the approximation (2.11), remains an interesting problem.

There are other estimates for the relaxation time τ. From microwave absorption[5] in Ge at a frequency $\omega=3.5\times10^{10}$ sec^{-1}, and $n\sim6\times10^{16}$ cm^{-3}, it is found that $\tau=7\times10^{-11}\,(1+0.086T^2)^{-1}$ sec, which at $T=1.5$ K is 6×10^{-11} sec. In this experiment the frequency and the carrier density are much smaller than in the ultrasonic experiment. For electron-hole liquids in Ge at the same density as the present analysis, several electromagnetic experiments have been performed. Values comparable to ours, $\tau=(2.2-2.6)\times10^{-13}$ sec, are deduced from the width of far-infrared absorption[14-16] at $\omega=(1.3-1.4)\times10^{13}$ sec^{-1}, which is 1 order of magnitude higher than the ultrasonic experiment. The magnetoplasma resonance experiments[17,18] at the same frequency range as the ultrasonic experiment give $\tau=(2-7)\times10^{-12}$ sec depending on the resonance frequency. The relaxation times obtained in the electromagnetic experiments agree with Rice's estimate[4] $\tau^{-1}\sim0.1\hbar\omega^2/E_F$, where $E_F=6.4$ meV is the sum of the electron and hole Fermi energies. The relaxation time we have obtained is much smaller than this value. The apparent discrepancy can be explained as follows. The quantity measured in the electromagnetic experiments is τ in the dielectric constant or

in the conductivity and mainly due to the electron-hole interband scattering,[4,15] which we have neglected in our calculation. If the Fermi sea were spherical, the intraband electron scattering, which is the origin of our τ, would not contribute to the damping of current. Therefore it is natural that the relaxation time measured in the electromagnetic resonance experiments is much longer than that measured in the ultrasonic experiment. Moreover, the spatial variation in the electromagnetic experiments is over scales much longer than k_F^{-1}, in contrast to the ultrasonic experiment. Without more detailed theory of the relaxation time, we cannot make a quantitative comparison between the relaxation times deduced from the different types of experiments.

ACKNOWLEDGMENTS

The authors would like to thank Professor J. P. Wolfe and Dr. S. J. Kirch for extensive discussions of their experiment and of electron-hole liquids in general. This research was supported in part by the National Science Foundation under Grants No. DMR-81-17182 and No. DMR-84-15063 and Materials Research Laboratory Program Grant No. DMR-80-20250, and by the Division of Materials Science, U.S. Department of Energy, under Contract No. DE-AC02-76ER01198.

APPENDIX

In this appendix we define several dimensionless functions derived from integrations over an ellipsoidal Fermi sea. The energy spectrum of electron is assumed to be of the form

$$\varepsilon(p)=\frac{p_x^2}{2m_x}+\frac{p_y^2}{2m_y}+\frac{p_z^2}{2m_z}\ . \tag{A1}$$

For application to the cases discussed in Secs. II and III, one should set $m_x=m_y=m_z=m$, and $m_x=m_y=m_\perp$ and $m_z=m_\parallel$, respectively.

The first function we define is related to the Lindhard function, but with finite relaxation time,

$$\int d\Lambda\frac{n^0_{\mathbf{p}-\hbar\mathbf{k}/2}-n^0_{\mathbf{p}+\hbar\mathbf{k}/2}}{\omega-\mathbf{v}\cdot\mathbf{k}+i/\tau}\ ,$$

where

$$\mathbf{v}=(p_x/m_x,p_y/m_y,p_z/m_z)\ .$$

We scale each component of momentum by the corresponding Fermi momentum and energy by the Fermi energy

$$\tilde{\mathbf{p}}=\left[\frac{p_x}{p_{Fx}},\frac{p_y}{p_{Fy}},\frac{p_z}{p_{Fz}}\right],$$
$$k=\left[\frac{k_x}{k_{Fx}},\frac{k_y}{k_{Fy}},\frac{k_z}{k_{Fz}}\right], \tag{A2}$$
$$\tilde{\omega}=\hbar\omega/\varepsilon_F,\quad \tilde{\tau}=\varepsilon_F\tau/\hbar\ .$$

The scaled dimensionless quantities are always indicated by tildes. Then with the help of the relation $n=p_{Fx}p_{Fy}p_{Fz}/3\pi^2\hbar^3$, the integral is represented by a dimensionless function

$$\frac{1}{\hbar}\int d\Lambda\frac{n^0_{\mathbf{p}-\hbar\mathbf{k}/2}-n^0_{\mathbf{p}+\hbar\mathbf{k}/2}}{\omega-\mathbf{v}\cdot\mathbf{k}+i/\tau}=\frac{3n}{2\varepsilon_F}\frac{1}{2\pi}\left[\int_{\tilde{\Omega}_1}d^3\tilde{p}-\int_{\tilde{\Omega}_2}d^3\tilde{p}\right]\frac{1}{\tilde{\omega}-2\tilde{\mathbf{p}}\cdot\tilde{\mathbf{k}}+i/\tilde{\tau}}\equiv\frac{3n}{2\varepsilon_F}L(\tilde{k},\tilde{\omega};\tilde{\tau})\ , \tag{A3}$$

where the integration is done over the region, for $\tilde{\Omega}_1$,

$$\left[\tilde{p}_x-\frac{\tilde{k}_x}{2}\right]^2+\left[\tilde{p}_y-\frac{\tilde{k}_y}{2}\right]^2+\left[\tilde{p}_z-\frac{\tilde{k}_z}{2}\right]^2\le 1\ ,$$

and for $\tilde{\Omega}_2$, (A4)

$$\left[\tilde{p}_x+\frac{\tilde{k}_x}{2}\right]^2+\left[\tilde{p}_y+\frac{\tilde{k}_y}{2}\right]^2+\left[\tilde{p}_z+\frac{\tilde{k}_z}{2}\right]^2\le 1\ .$$

The second function we define is the integration of the velocity,

$$\frac{1}{\hbar}\int d\Lambda\frac{n^0_{\mathbf{p}-\hbar\mathbf{k}/2}-n^0_{\mathbf{p}+\hbar\mathbf{k}/2}}{\omega-\mathbf{v}\cdot\mathbf{k}+i/\tau}\mathbf{v}=\frac{3n}{2\varepsilon_F}\frac{1}{2\pi}\left[\int_{\tilde{\Omega}_1}d^3\tilde{p}-\int_{\tilde{\Omega}_2}d^3\tilde{p}\right]\frac{1}{\tilde{\omega}-2\tilde{\mathbf{p}}\cdot\tilde{\mathbf{k}}+i/\tilde{\tau}}(v_{Fx}\tilde{p}_x,v_{Fy}\tilde{p}_y,v_{Fz}\tilde{p}_z)$$
$$=\frac{3n}{2\varepsilon_F}J(\tilde{k},\tilde{\omega};\tilde{\tau})\left[v_{Fx}\frac{\tilde{k}_x}{\tilde{k}},v_{Fy}\frac{\tilde{k}_y}{\tilde{k}},v_{Fz}\frac{\tilde{k}_z}{\tilde{k}}\right], \tag{A5}$$

where $J(\tilde{k};\tilde{\omega};\tilde{\tau})$ is defined as

$$J(\tilde{k},\tilde{\omega};\tilde{\tau})\equiv\frac{1}{2\pi}\left[\int_{\tilde{\Omega}_1}d^3\tilde{p}-\int_{\tilde{\Omega}_2}d^3\tilde{p}\right]\frac{\tilde{\mathbf{p}}\cdot\hat{\mathbf{k}}}{\tilde{\omega}-2\tilde{\mathbf{p}}\cdot\tilde{\mathbf{k}}+i/\tilde{\tau}}\ . \tag{A6}$$

When the collision time τ is infinite, the function L becomes the Lindhard function, in dimensionless form,

$$L(\tilde{k},\tilde{\omega};\infty)=\frac{1}{2\pi}\left[\int_{\tilde{\Omega}_1}d^3\tilde{p}-\int_{\tilde{\Omega}_2}d^3\tilde{p}\right]\frac{1}{\tilde{\omega}-2\tilde{\mathbf{p}}\cdot\tilde{\mathbf{k}}+i\delta}\ , \tag{A7}$$

and the function J becomes

$$J(\tilde{k},\tilde{\omega};\infty)=\frac{1}{2\pi}\left[\int_{\tilde{\Omega}_1}d^3\tilde{p}-\int_{\tilde{\Omega}_2}d^3\tilde{p}\right]\frac{\tilde{\mathbf{p}}}{\tilde{\omega}-2\tilde{\mathbf{p}}\cdot\tilde{\mathbf{k}}+i\delta}\cdot\frac{\tilde{\mathbf{k}}}{\tilde{k}}=\frac{1}{2\pi}\left[\int_{\tilde{\Omega}_1}d^3\tilde{p}-\int_{\tilde{\Omega}_2}d^3\tilde{p}\right]\frac{1}{2\tilde{k}}\left[-1+\frac{\tilde{\omega}}{\tilde{\omega}-2\tilde{\mathbf{p}}\cdot\tilde{\mathbf{k}}+i\delta}\right]$$
$$=\frac{\tilde{\omega}}{2\tilde{k}}L(\tilde{k},\tilde{\omega};\infty)\ . \tag{A8}$$

For $\omega=ck$ ($c<v_F$) and $k\to 0$, $L(\tilde{k},\tilde{\omega};\infty)$ becomes

$$L(\tilde{k}\to 0,2c\tilde{k}/v_F;\infty)=-\left[1+\frac{c}{2v_F}\ln\left|\frac{1-c/v_F}{1+c/v_F}\right|\right]-i\frac{\pi}{2}\frac{c}{v_F}\ . \tag{A9}$$

When the wave number is very small, $k\ll k_F$, the functions L and J become the integrals which appear in Pippard's theory[2] of sound attenuation in metals. In this case the difference of the integral operators becomes an integral of a δ function:

$$\int_{\tilde{\Omega}_1}d^3\tilde{p}-\int_{\tilde{\Omega}_2}d^3\tilde{p}=\int d^3\tilde{p}\,\delta(\tilde{p}-1)\tilde{\mathbf{p}}\cdot\tilde{\mathbf{k}}\ .$$

Therefore (A3) and (A6) reduce to

$$L(\tilde{k}\to 0,\tilde{\omega};\tilde{\tau})=\int_{-1}^{1}dx\frac{\tilde{k}x}{\tilde{\omega}-2\tilde{k}x+i/\tilde{\tau}}=-iaI_1(a)\ , \tag{A10}$$

$$J(\tilde{k}\to 0,\tilde{\omega};\tau)=\int_{-1}^{1}dx\frac{\tilde{k}x^2}{\tilde{\omega}-2\tilde{k}x+i/\tilde{\tau}}=-iaI_2(a)\ , \tag{A11}$$

where

$$a=\frac{2\tilde{k}\tilde{\tau}}{1-i\tilde{\omega}\tilde{\tau}}=\frac{kv_F\tau}{1-i\omega\tau}\ , \tag{A12}$$

and $I_n(a)$ is defined as

$$I_n(a)=\frac{1}{2}\int_{-1}^{1}dx\frac{x^n}{1+iax}\ . \tag{A13}$$

The first three $I_n(a)$ are important:

$$I_0(a)=\frac{1}{a}\tan^{-1}a\ , \tag{A14}$$

$$I_1(a)=\frac{1}{ia^2}(a-\tan^{-1}a)=\frac{1}{ia}[1-I_0(a)]\ , \tag{A15}$$

$$I_2(a)=\frac{1}{a^3}(a-\tan^{-1}a)=\frac{1}{a^2}[1-I_0(a)]\ . \tag{A16}$$

The integrals containing $\partial n^0/\partial\varepsilon$ are expressed in terms of these functions as follows:

$$\int d\Lambda\left[-\frac{\partial n^0}{\partial\varepsilon}\right]\frac{\delta\mu}{\omega-\mathbf{v}\cdot\mathbf{k}+i/\tau}=\frac{3n}{2\varepsilon_F}\delta\tilde{\mu}\frac{\hbar}{2\pi}\int d^3\tilde{p}\,\delta(\tilde{\varepsilon}-1)\frac{1}{\tilde{\omega}-2\tilde{\mathbf{p}}\cdot\tilde{\mathbf{k}}+i/\tilde{\tau}}=-i\frac{3n}{2\varepsilon_F}\delta\mu\frac{\tau}{1-i\tilde{\omega}\tilde{\tau}}I_0(a)\ , \tag{A17}$$

$$\int d\Lambda\left[-\frac{\partial n^0}{\partial\varepsilon}\right]\frac{\mathbf{u}\cdot\mathbf{p}}{\omega-\mathbf{v}\cdot\mathbf{k}+i/\tau}=\frac{3n}{2\varepsilon_F}\frac{\hbar}{2\pi}\int d^3\tilde{p}\,\delta(\tilde{\varepsilon}-1)\frac{2\tilde{\mathbf{p}}\cdot\tilde{\mathbf{k}}}{\tilde{\omega}-2\tilde{\mathbf{p}}\cdot\tilde{\mathbf{k}}+i/\tilde{\tau}}=-i\frac{3n}{2\varepsilon_F}\frac{2\tilde{k}\tilde{\tau}}{1-i\tilde{\omega}\tilde{\tau}}I_1(a)\ , \tag{A18}$$

where the second equality of (A18) holds only when $\tilde{\boldsymbol{\kappa}}\|\tilde{\mathbf{k}}$. Under the same condition ($\tilde{\boldsymbol{\kappa}}\|\tilde{\mathbf{k}}$) we also have

$$\int d\Lambda\left[-\frac{\partial n^0}{\partial\varepsilon}\right]\frac{\delta\mu}{\omega-\mathbf{v}\cdot\mathbf{k}+i/\tau}\mathbf{v}=\frac{3n}{2\varepsilon_F}\delta\tilde{\mu}\frac{1}{2\pi}\int d^3\tilde{p}\,\delta(\tilde{\varepsilon}-1)\frac{\tilde{\mathbf{p}}}{\tilde{\omega}-2\tilde{\mathbf{p}}\cdot\tilde{\mathbf{k}}+i/\tilde{\tau}}\cdot\frac{\tilde{\mathbf{k}}}{\tilde{k}}\left[v_{Fx}\frac{\tilde{k}_x}{\tilde{k}},v_{Fy}\frac{\tilde{k}_y}{\tilde{k}},v_{Fz}\frac{\tilde{k}_z}{\tilde{k}}\right]$$
$$=-i\frac{3n}{2\varepsilon_F}\delta\mu\frac{\tau}{1-i\tilde{\omega}\tilde{\tau}}I_1(a)\left[v_{Fx}\frac{\tilde{k}_x}{\tilde{k}},v_{Fy}\frac{\tilde{k}_y}{\tilde{k}},v_{Fz}\frac{\tilde{k}_z}{\tilde{k}}\right]\ , \tag{A19}$$

$$\int d\Lambda\left[-\frac{\partial n^0}{\partial\varepsilon}\right]\frac{\mathbf{u}\cdot\mathbf{p}}{\omega-\mathbf{v}\cdot\mathbf{k}+i/\tau}\mathbf{v}=\frac{3n}{2\varepsilon_F}\frac{\hbar}{2\pi}\int d^3\tilde{p}\,\delta(\tilde{\varepsilon}-1)\frac{2\tilde{\mathbf{p}}\cdot\tilde{\mathbf{k}}}{\tilde{\omega}-2\tilde{\mathbf{p}}\cdot\tilde{\mathbf{k}}+i/\tilde{\tau}}(v_{Fx}\tilde{p}_x,v_{Fy}\tilde{p}_y,v_{Fz}\tilde{p}_z)$$
$$=-i\frac{3n}{2\varepsilon_F}\hbar\frac{2\tilde{k}\tilde{\tau}}{1-i\tilde{\omega}\tilde{\tau}}I_2(a)\left[v_{Fx}\frac{\tilde{k}_x}{\tilde{k}},v_{Fy}\frac{\tilde{k}_y}{\tilde{k}},v_{Fz}\frac{\tilde{k}_z}{\tilde{k}}\right]\ . \tag{A20}$$

*Present address: The Research Institute for Iron, Steel and Other Metals, Tohoku University, 2-1-1 Katahira, Sendai 980, Japan.

[1]W. Dietsche, S. J. Kirch, and J. P. Wolfe, Phys. Rev. B **26**, 780 (1982).

[2]A. B. Pippard, Philos. Mag. **46**, 1104 (1955).

[3]For example, see C. Kittel, *Quantum Theory of Solids* (Wiley, New York, 1963), Chap. 17.

[4]For a review, see T. M. Rice, in *Solid State Physics,* edited by H. Ehrenreich, F. Seitz, and D. Turnbull (Academic, New York, 1977), Vol. 32; J. C. Hensel, G. A. Thomas, and T. G. Phillips, *ibid.*

[5]Estimates of various relaxation times are summarized in T. Ohyama, I. Honbori, and E. Otsuka, J. Phys. Soc. Jpn. **48**, 1559 (1980).

[6]A reversed problem is the damping of electron-hole droplet motion by phonon scattering. See D. S. Pan, D. L. Smith, and T. C. McGill, Phys. Rev. B **17**, 3284 (1978), and the references therein.

[7]J. Bardeen and W. Shockley, Phys. Rev. **80**, 72 (1950).

[8]L. P. Kadanoff and G. Baym, *Quantum Statistical Mechanics* (Benjamin, Reading, MA 1962).

[9]E. M. Conwell, *High Field Transport in Semiconductors,* Suppl. 9 of *Solid State Physics* (Academic, New York, 1967).

[10]C. Herring and E. Vogt, Phys. Rev. **101**, 944 (1956). The notations of deformation potentials in our paper, except Ξ_d and Ξ_u, are not conventional.

[11]K. Murase, K. Enjouji, and E. Otsuka, J. Phys. Soc. Jpn. **29**, 1248 (1970).

[12]The actual band structure and corresponding deformation potentials are complicated, and the relevant values (shifts of the band edges due to dilatation) are not well known [see H. Fujiyasu, K. Murase, and E. Otsuka, J. Phys. Soc. Jpn. **29**, 685 (1970)]. Although the value used here for Ge is somewhat arbitrary, the resultant effects of the uncertainty are not too large since $|\Xi_1|$ and $|\Xi_3|$ are much larger than $|\Xi_h|$. For Si, Ξ_h is more ambiguous, and the result is more sensitive to Ξ_h since $|\Xi_1| \sim |\Xi_h|$. Therefore the result (Fig. 5) should be considered tentative.

[13]R. S. Markiewicz, Phys. Status Solidi B **83**, 659 (1977). The argument in this paper that only the dilatational part, $\Xi_d + \Xi_u/3$, is screened does not hold, and one should treat the three components separately. Therefore the resultant screened deformation potentials are not reliable.

[14]V. N. Murzin, V. A. Zayats, and V. L. Kononenko, Fiz. Tverd. Tela (Leningrad) **17**, 2684 (1975) [Sov. Phys.—Solid State **17**, 1783 (1976)]; V. S. Vavilov, V. A. Zayats, and V. N. Murzin, Pis'ma Zh. Eksp. Teor. Fiz. **10**, 304 (1969) [JETP Lett. **10**, 192 (1969)].

[15]J. H. Rose, H. B. Shore, and T. M. Rice, Phys. Rev. B **17**, 752 (1978).

[16]H. G. Zarate and T. Timusk, Phys. Rev. B **19**, 5223 (1979).

[17]V. I. Gavrilenko, V. L. Kononenko, T. S. Mandel'shtam, and V. N. Murzin, Pis'ma Zh. Eksp. Teor. Fiz. **23**, 701 (1976) [JETP Lett. **23**, 645 (1976)].

[18]K. Muro and Y. Nisida, J. Phys. Soc. Jpn. **40**, 1069 (1976).